Adaptive Optimal Control Algorithm for Maturing Energy Management Strategy in Fuel-Cell/Li-ion-Capacitor Hybrid Electric Vehicles

Chen-Hong Zheng[1], Chao-Ming Lee[2]
Department of Electrical Engineering,
National Taiwan University, Taipei, Taiwan
[1]wmycode@yahoo.com.tw; [2]neumann0818@gmail.com

Yu-Chun Huang[3], Wei-Song Lin[4]
Department of Electrical Engineering,
National Taiwan University, Taipei, Taiwan
[3]caca912@hotmail.com; [4]weisong@cc.ee.ntu.edu.tw

***Abstract*—Energy management in a fuel cell/Li-ion capacitor hybrid vehicle needs to determine appropriate power split among the load and distinct power sources in order to minimize fuel consumption and power fluctuations in the fuel cell system while supplying adequate power to the load, and the state-of-charge of the Li-ion capacitor maintained at the permissible levels. This paper formulates this case as a problem of fuel minimization subject to mixed equality and inequality constraints imposed by the dynamics and operational limitations of the fuel cell and Li-ion capacitor. Then the adaptive optimal control algorithm is proposed to automatically draw out the best energy management strategy via reinforcement learning and sequential optimization in standard driving cycles. The results of testing the algorithm in a fuel cell/Li-ion capacitor hybrid sedan verifies the efficacy of the proposed design in energy saving.**

Keywords—adaptive optimal control algorithm; energy management; fuel cell hybrid power system; electric vehicle

I. INTRODUCTION

A Fuel-cell/Li-ion capacitor Hybrid Power System (FHPS) for an electric vehicle hybridizes a proton-exchange-membrane Fuel Cell System (FCS) with a bank of Li-ion capacitors to supply electric power and retrieve regenerative electricity. The FCS generates electric power directly from hydrogen, but a reverse power flow is impossible. Li-ion capacitor is a state-of-the-art supercapacitor, which features a higher energy density and a very small leakage in comparison with electrical-double-layer capacitor [1, 2]. In the FHPS, Li-ion capacitors provide a reservoir for the regenerative electricity. Rapid load variations which may induce oxygen starvation and thereby cause permanent damage to the proton-exchange membranes of the fuel cell are shared by Li-ion capacitors. This makes the FHPS with both high power and energy densities, and the power-capacity rating of the FCS is required to meet the average demand only, rather than the peak demand [3, 4]. In powering electric vehicle, the FHPS is more cost-effective and energy-efficient than using the fuel cell alone.

The FHPS relies on a good Energy Management Strategy (EMS) to appropriately distribute power among the load and distinct power sources. In general, the design methods of the EMS reported in literature can be categorized into the analysis approach and the optimization approach. Basically, the analysis approach is an application of the control technique to achieve better energy efficiency. Baisden et al. [5] presented a three-operation-mode control strategy to define the output power of each source. Andersson et al. [6] proposed a low-pass filter control strategy to charge the supercapacitor while neglecting the plant dynamics. Haifang et al. [7] improved the low-pass filter control strategy by taking into account the vehicle speed and the State-of-Charge (SoC) of supercapacitor. Vahidi et al. [8] employed a model-predictive control methodology to develop a current management strategy which could overcome the problem of oxygen starvation, air compressor surge, and choke in the FCS. Chen et al. [9] used a multiple-model, predictive control for the optimization of power usage and control of oxygen. Zhu et al. [10] adopted a cluster-weighted modeling algorithm to recognize the load transient and determine the power-split between the FCS and Energy Storage System (ESS). Use of fuzzy logic based EMS was reported in [11-13].

The optimization approach tries to draw out the best EMS through a procedure of optimization. Based on the equivalent consumption minimization strategy, Paganelli [14] and Rodatz et al. [15] presented a local optimal scheme in which the cost function was evaluated based on hydrogen consumption and equivalent fuel consumption of the ESS. However, the local optimization does not necessarily guarantee the same conclusion in global viewpoint. Besides, operating restrictions of each power devices in the hybrid system are not ensured to protect them from ill conditions which may damage device or degrade life time. Feroldi et al. [16] developed three energy management strategies, based on the efficiency curve of fuel cell, for electric vehicles powered by hybrid power systems. One of the strategies was attained by utilizing a constrained nonlinear programming method. Other strategies were attained by analysis on empirical observations. Delprat and Bernard [17, 18] matured the EMS by forward iteration of a state equation, a costate equation, and a stationary equation with an assumption that the initial costate vector was available. This approach is a non-causal solution because the entire driving cycle must be available before application of the initial costate vector, and the convergence of the algorithm is sensitive to parameter errors. Lin and Zheng [4] made use of a procedure of reinforcement learning [19, 20] and sequential optimization to mature the EMS of a fuel-cell/electrical-double-layer-capacitor hybrid power system. The procedure is referred to as the Adaptive

This work was supported in part by National Science Council and National Taiwan University, Taiwan under grants NSC101-2221-E-002-039 and 101R30401-2.

978-1-4673-5769-2/13/$31.00 ©2013 IEEE

Optimal Control Algorithm (AOCA). The theory and convergence proof of the AOCA refers to [21, 22]. Basically, the AOCA inherits the concept of Dual Heuristic Programming (DHP), a version of approximate dynamic programming [23]. Particularly, the AOCA formulates the optimality conditions and the learning/optimization laws with Pontryagin's minimum (maximum) principle [24], rather than by taking derivative over the Hamiltonian-Jacobi-Bellman (HJB) equation [25] like that DHP did. This paper presents the entire design of the AOCA dedicated to automatically mature the EMS of fuel-cell/Li-ion-capacitor hybrid vehicle in the interested driving cycles. Since the dynamics and operational limitations of Li-ion capacitor is different from that of electrical-double-layer capacitor, the AOCA presented in this paper is distinct from that presented in [4].

The organization of the paper is as follows. Section II formulates the fuel minimization problem of FHPS supplying an electric vehicle. Section III elaborates the AOCA. Section IV tests the AOCA in the energy management of a fuel-cell/Li-ion-capacitor hybrid sedan. Finally, conclusion is drawn in Section V. The nomenclature lists the symbols used in the text.

NOMENCLATURE

$\dot{m}_{H_2}$	Hydrogen-consumption rate of the FCS, in units of gs^{-1}.
P_{ESS}	Power at the terminal nodes of the ESS.
P_{FC}	Output power of the FCS, in units of 100 kW.
P_L	Power at the input terminal of the direct torque control driver.
$\mathcal{P}_L^i$	The sequence of power demands associated with driving cycle i.
P_C	Power out of C of the nominal model for Li-ion capacitor.
$x = E/E_{\max}$	State of charge (SoC) of the ESS; E the energy, $E_{\max}$ the maximum energy stored in the ESS.
u_k	$u_k \triangleq$ desired $P_{FC,k}$; desired output power of the FCS.
η_1	Efficiency of the boost converter.
η_2	Efficiency of the buck/boost converter.
f(·)	The SoC dynamics of the ESS.
J(·)	Cost function.
$\mathcal{U}(\cdot\|\alpha)$	EMS (neural) network; $\alpha = \{\alpha_1, \cdots, \alpha_{n_\alpha}\}$ the free parameters.
$\Lambda(\cdot\|\beta)$	Lag judgment (neural) network; $\beta = \{\beta_1, \cdots, \beta_{n_\beta}\}$ the free parameters.
$\Lambda^\circ(\cdot\|\beta)$	Lead judgment (neural) network.
k	Index for time step.
K	Total time steps pertaining to a driving cycle.
τ	Sampling period.
$*$	Indicating an optimum.
θ_i	Penalty constant

II. THE FUEL MINIMIZATION PROBLEM OF FHPS

Fig. 1 is the layout of the concerned FHPS supplying an electric vehicle. The Induction Motor (IM) associated with the direct torque control driver [26] propels the front wheels through the reduction gear and differential gear. The FHPS hybridizes a proton-exchange-membrane FCS with an ESS consisting of Li-ion capacitors. A unidirectional boost converter interfaces the FCS to the dc bus, and protects the FCS from damaged by reverse current. The ESS employs a bidirectional buck-boost converter to allow a bidirectional power flow, in which case the ESS is able not only to deliver the shared power but also to retrieve regenerative electricity [4]. The converters are under control of the power split controller (PSC). Control strategies of the FHPS have to deal with power management which determines appropriate power split between the direct torque control driver and the distinct power sources to minimize hydrogen consumption [27], while staying within specified constraints on drivability, reliability, Li-ion capacitor sustenance, etc. The EMS is responsible for directing the PSC to achieve the best power split so that the hydrogen consumption and power fluctuations in the FCS would be minimized while supplying adequate power to the load, and the SoC of the ESS maintained at the permissible levels. We assume that the PSC loop responds much faster than the EMS loop such that the EMS can neglect transients incurred by the switching devices of the converters. The AOCA is a training agent of the EMS (neural) network (see Fig. 3), which tries to draw out the best EMS through reinforcement learning and sequential optimization in the interested driving cycles.

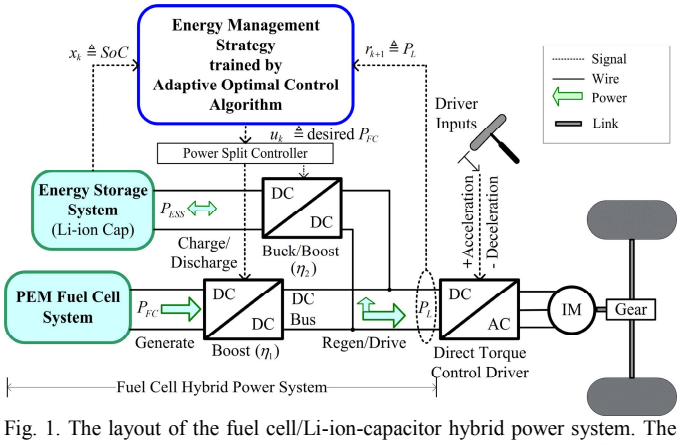

Fig. 1. The layout of the fuel cell/Li-ion-capacitor hybrid power system. The energy management strategy directs the power split controller to split power between the ESS and FCS. The adaptive optimal control algorithm tries to draw out the best energy management strategy.

Optimization of the EMS in a driving cycle for energy saving can be formulated as the fuel minimization problem:

For $P_{L,k} \in \mathcal{P}_L^i$, $k = 0, 1, \cdots, K-1$, and $i = 1, \cdots, I$,

$$\min_{\alpha} \mathrm{J}(x_0 | \alpha) = \min_{\alpha} \left\{ \mathrm{J}(x_K, \alpha^* | \theta) + \sum_{k=0}^{K-1} [\dot{m}_{H_2}(u_k)\tau] \right\} \tag{1}$$

subject to

$$x_{k+1} = \mathrm{f}(x_k, P_{L,k}, u_k), \tag{2}$$

$$u_k = \mathcal{U}(x_k, P_{L,k} | \alpha), \tag{3}$$

and the operational limitations of the FCS and ESS listed in (4) through (7).

1) $P_{FC,k}\eta_1 + P_{ESS,k}\eta_2 = P_{L,k}$. (4)

The energy conservation principle must be satisfied.

2) $P_{FC_{\min}} \le P_{FC,k} \le P_{FC_{\max}}$. (5)

The lower power limitation, $P_{FC_{\min}}$ (> 0), is needed because the FCS cannot store electrical energy. In the high-power operation of the FCS, the maximum power that can be drawn

is limited to the rated value ($P_{FC\max}$) since excessive output power may lead to oxygen starvation and gas flow chaos that would damage the FCS.

3) $\Delta P_{FC,fall} \le \dfrac{d}{dt} P_{FC,k} \le \Delta P_{FC,rise}$. (6)

This constraint means that the rate of change in the FCS power also should be limited to assure that the air compressor (which has a slow dynamic response) can cope with the power fluctuations.

4) $SoC_{\min} \le x_k \le SoC_{\max}$. (7)

The upper bound of the SoC ($SoC_{\max}$) of the ESS is chosen somewhat smaller than unity for safety considerations. The lower bound of the SoC ($SoC_{\min}$) is necessary because there is a lower bound for the voltage of Lithium-ion capacitor.

III. Adaptive Optimal Control Algorithm for Fuel Cell/Li-ion-Capacitor Hybrid Power System

This section elaborates the AOCA dedicated to mature the EMS of the FHPS in a number of standard driving cycles.

A. The Augmented Fuel Minimization Problem

Define the soft penalty function, $h_i(g_i)$, as

$$h_i(g_i) = 1 - \frac{1}{1+\exp[c(g_i - b_i)]} + \frac{1}{1+\exp[c(g_i - a_i)]}, \quad (8)$$

where g_i is the argument, and c is a large positive number referred to as the slope constant. It is easy to show that

$$h_i(g_i) = 1 - \frac{1}{1+\exp[c(g_i - b_i)]} \text{ as } a_i \to -\infty, \quad (9)$$

$$h_i(g_i) = \frac{1}{1+\exp[c(g_i - a_i)]} \text{ as } b_i \to \infty, \quad (10)$$

and $0 \le h_i(g_i) \le 0.5$ as $a_i \le g_i \le b_i$, otherwise $0.5 < h_i(g_i) \le 1$. When $c \to \infty$ we get $h_i(g_i) = 0$ for $a_i \le g_i \le b_i$, and otherwise $h_i(g_i) = 1$.

Define the augmented local cost function, ϕ_k , as

$$\phi_k \triangleq \phi(k, x_k, u_k, r) = \dot{m}_{H_2}(u_k)\tau + \frac{1}{2}\sum_{i=1}^{\upsilon}\left[\theta_i h_i\left(g_{i,k}\right) g_{i,k}^2\right], \quad (11)$$

where r is the reference input, $\triangleq$ defines by equality, $\theta_i \in \theta \triangleq \{\theta_1, \cdots, \theta_\upsilon\}$ is referred to as the penalty constant, and the soft penalty functions $h_i(g_i)$ $i = 1, \cdots, \upsilon\,(=3)$, encode the following parameters:

g_i	a_i	b_i	c
Eqn. (5): $g_1 = u_k$	$P_{FC\min}$	$P_{FC\max}$	large value
Eqn. (6): $g_2 = u_k - u_{k-1}$	$\Delta P_{FC,fall}\tau$	$\Delta P_{FC,rise}\tau$	large value
Eqn. (7): $g_3 = x_k$	$SoC_{\min}$	$SoC_{\max}$	large value

Then, the augmented fuel minimization problem can be formulated as in (12) through (14).

For $P_{L,k} \in \mathcal{P}_L^i$, $k = 0, 1, \cdots, K-1$, and $i = 1, \cdots, I$,

$$\min_{\alpha} \mathrm{J}(x_0, \alpha \,|\, \theta) = \min_{\alpha}\left\{\mathrm{J}(x_K, \alpha^* \,|\, \theta) + \sum_{k=0}^{K-1}\phi(k, x_k, u_k, r)\right\} \quad (12)$$

subject to:

$$x_{k+1} = \mathrm{f}(x_k, P_{L,k}, u_k), \quad (13)$$

$$u_k = \mathcal{U}\left(x_k, P_{L,k} \,|\, \alpha\right). \quad (14)$$

The exterior penalty function method [28] has shown that, as $c \to \infty$ and $\theta_i \to \infty$ for $i = 1, \cdots, \upsilon\,(=3)$, the optimum of the augmented fuel minimization problem is identical to that of the fuel minimization problem.

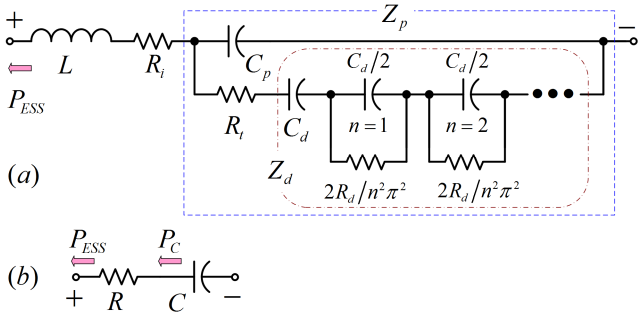

Fig. 2. The equivalent circuit and nominal model for Li-ion capacitor. (a) The equivalent circuit [2]. (b) The nominal model used.

B. Nominal Models of the FCS and ESS

If the gas pressure, stack temperature and humidity are all well-regulated inside the FCS then fitting the hydrogen-consumption rate with the third-order polynomial function leads to the nominal model of performance [29-32]:

$$\dot{m}_{H_2}(P_{FC}) = a_3 P_{FC}^3 + a_2 \cdot P_{FC}^2 + a_1 \cdot P_{FC} + a_0, \quad (15)$$

where P_{FC} in units of 100 kW is the output power of the FCS, $\dot{m}_{H_2}$ in units of gs^{-1} is the hydrogen-consumption rate, and (a_3 , a_2 , a_1 , a_0)= (4.1953, -2.0662, 1.6944, 0.0066) will be used in the tests. Additionally, usage of the FCS model is subject to a number of operational limitations shown in (4) through (7).

Li-ion capacitor features a high energy density and a high power density [2, 33] that makes it suitable for assisting the FCS in supplying urgent power demand and capturing regenerative electricity. But the permissible voltage range for Li-ion capacitor is generally [2.2, 3.8] V that sets an operational limitation to the SoC between 33% and 100%. The equivalent circuit for Li-ion capacitor comprises of three series components as shown in Fig. 2(a). The three components represent in line impedance, L, series resistance, R_i , and transfer impedance Z_p [2]. The transfer impedance is equivalent to a double layer capacitor C_p in parallel with limiting resistance R_t in series with a diffusion impedance Z_d . The nominal model used in the gradient decent method is the series connection of R and C as shown in Fig. 2(b) , where

$$R = R_i + R_t + 0.3022 \times R_d, \; C = C_p + C_d, \quad (16)$$

and where $0.3022R_d$ is the diffusion resistance for $n=6$.

Using the nominal model, the charge-discharge contour plot of the ESS takes the form:

$$P_C(x,P_{ESS})=\left(1-\sqrt{1-\frac{2RC}{x\,E_{\max}}P_{ESS}}\right)\frac{x\,E_{\max}}{RC}. \tag{17}$$

Therefore, the SoC dynamics of the ESS can be approximately described by the first-order difference equation:

$$x_{k+1}=x_k-P_C\left(x_k,P_{ESS,k}\right)\frac{\tau}{E_{\max}}, \tag{18}$$

where τ is the sampling period. Taking into account the equality constraint shown in (4), equation (18) should be written as

$$x_{k+1}=x_k-P_C\left(x_k,\frac{P_{L,k}-u_k\eta_1}{\eta_2}\right)\frac{\tau}{E_{\max}}. \tag{19}$$

C. Optimality Conditions for the AOCA

For simplicity, denote $\mathrm{J}_k\triangleq\mathrm{J}(x_k|\theta)$, $\mathrm{J}_K^*\triangleq\mathrm{J}(x_K,\alpha^*|\theta)$, $\phi_k\triangleq\phi(k,x_k,u_k,r)$ and $\mathrm{f}_k\triangleq\mathrm{f}(x_k,P_{L,k},u_k)$. Then, the objective function shown in (12) can be written

$$\min_{\alpha}\mathrm{J}(x_0|\theta)=\min_{\alpha}\left\{\mathrm{J}_K^*+\sum_{k=0}^{K-1}\phi_k\right\}. \tag{20}$$

The cost function in the 'min' operation of (20) is

$$J_0=J_K^*+\sum_{k=0}^{K-1}\phi_k. \tag{21}$$

Define a costate λ (i.e., Lagrange multiplier) [34], which is an as yet undetermined variable. Then we adjoin (21) with (13) to form the adjoined cost function:

$$J_{\mathrm{adj}}=J_K^*+\sum_{k=0}^{K-1}\left\{\vec{H}_k-x_{k+1}\lambda_{k+1}\right\}, \tag{22}$$

where $\vec{H}_k\triangleq\vec{H}(k,x_k,u_k,\lambda_{k+1})$ is the Hamiltonian function defined as

$$\vec{H}_k=\phi_k+\mathrm{f}_k\,\lambda_{k+1}\quad(k=0,1,\cdots,K-1). \tag{23}$$

Minimizing the adjoined cost function (22) by the calculus of variations leads to the necessary conditions for optimality:

$$x_{k+1}=\mathrm{f}_k \tag{24}$$

$$0=\frac{\partial\phi_k}{\partial u_k}+\left(\frac{\partial\mathrm{f}_k}{\partial u_k}\right)\lambda_{k+1}^*=\frac{\partial\vec{H}_k}{\partial u_k}\quad\text{(Stationary condition)} \tag{25}$$

$$\lambda_k^*=\frac{\partial\phi_k}{\partial x_k}+\left(\frac{\partial\mathrm{f}_k}{\partial x_k}\right)\lambda_{k+1}^*=\frac{\partial\vec{H}_k}{\partial x_k}\quad\text{(Costate equation)} \tag{26}$$

$$\left(\frac{\partial\phi_0}{\partial x_0}+\left(\frac{\partial\mathrm{f}_0}{\partial x_0}\right)\lambda_1^*\right)\hat{x}_0=0 \tag{27}$$

$$\left(\lambda_K^*-\frac{\partial J_K^*}{\partial x_K}\right)\hat{x}_K=0 \tag{28}$$

where $\hat{x}_K$ and $\hat{x}_0$ are arbitrary vector variables corresponding to the variations. Note that the costate equation develops backward-in-time. A proof of the necessary conditions refers to [35].

The AOCA can start at arbitrary time step so that x_0 and x_K must be free. When x_0 is free, (27) leads to

$$\frac{\partial\phi_0}{\partial x_0}+\left(\frac{\partial\mathrm{f}_0}{\partial x_0}\right)\lambda_1^*=0. \tag{29}$$

Substituting (29) into (26) yields $\lambda_0^*=0$ (i.e., the initial-point condition). When x_K is free, (28) leads to the end-point condition:

$$\lambda_K^*=\partial J_K^*/\partial x_K. \tag{30}$$

D. Learning/Optimization Laws of the AOCA

The discrete minimum principle [35] refers to the property that the Hamiltonian function is a minimum on an optimal trajectory. An optimization procedure trying to lead the system from (x_k,λ_k) to $(x_{k+1}^*,\lambda_{k+1}^*)$ needs to minimize the one-shot Hamiltonian function:

$$H_k=\phi_k+\mathrm{f}_k\,\lambda_{k+1}^*. \tag{31}$$

The gradients of H_k with respect to $\alpha_i\in\alpha$ and x_k can be written as in (32) and (33).

$$\gamma_{i,k}=\frac{\partial H_k}{\partial\alpha_i}=\left(\frac{\partial\mathcal{U}(x_k,P_{L,k}|\alpha)}{\partial\alpha_i}\right)z_k\qquad i=1,2,\ldots,n_\alpha, \tag{32}$$

$$\lambda_k^{\mathrm{D}}=\frac{\partial H_k}{\partial x_k}=\frac{\partial\phi_k}{\partial x_k}+\left(\frac{\partial\mathrm{f}_k}{\partial x_k}\right)\lambda_{k+1}^*+\left(\frac{\partial\mathcal{U}(x_k,P_{L,k}|\alpha)}{\partial x_k}\right)z_k, \tag{33}$$

where (33) is referred to as the back-projection equation, and

$$z_k=\frac{\partial H_k}{\partial u_k}=\frac{\partial\phi_k}{\partial u_k}+\left(\frac{\partial\mathrm{f}_k}{\partial u_k}\right)\lambda_{k+1}^*. \tag{34}$$

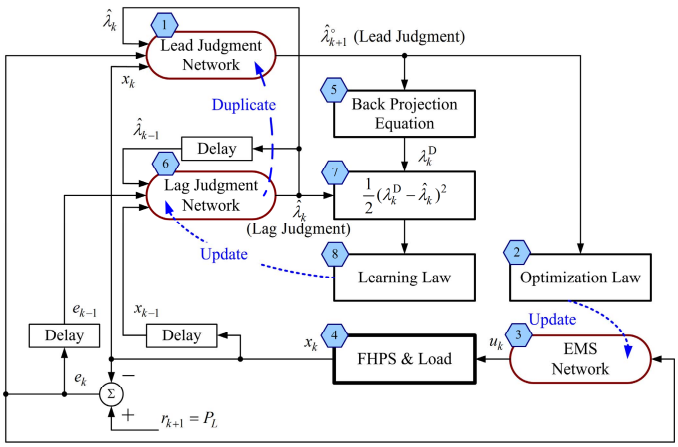

Fig. 3. The computation blocks pertaining to the AOCA. The numbered hexagon indicates the order of the corresponding block computed by the AOCA. The initial-point condition $\lambda_0^*=0$ leads to $\hat{\lambda}_0=0$.

Fig. 3 shows the computation blocks and the order of computation of the AOCA. In order to evaluate (33) and (34) forward-in-time, the lag judgment network $\Lambda(\cdot|\beta)$ and the judgment (neural) network $\Lambda^{\circ}(\cdot|\beta)$ cascade to estimate the optimal costate λ_{k+1}^*, where β is the free parameters. The AOCA carries out a learning law and an optimization law to

update α and β, respectively, aiming at achieving

$$\frac{1}{2}\sum_{k=0}^{K-1}\sum_{i=1}^{n_\alpha}\gamma_{i,k}^2 \le \varepsilon_\gamma \text{ and } \frac{1}{2}\sum_{k=0}^{K-1}(\lambda_k^{\mathrm{D}}-\hat{\lambda}_k)^2 \le \varepsilon_\lambda, \quad (35)$$

where $\varepsilon_\gamma, \varepsilon_\lambda > 0$ are defined tolerances. Convergence of the AOCA leads to

$$\lambda_k^* \approx \hat{\lambda}_k = \Lambda\left(x_{k-1}, \hat{\lambda}_{k-1}, e_{k-1} \middle| \beta\right), \quad \lambda_{k+1}^* \approx \hat{\lambda}_{k+1}^{\circ} = \Lambda^{\circ}\left(x_k, \hat{\lambda}_k, e_k \middle| \beta\right)$$

for each k, and the trained EMS network $\mathcal{U}(\cdot|\alpha)$ contains the best EMS. Notice that the learning law updates the parameter values associated with the lag judgment network. The lead judgment network just duplicates the corresponding parameter values of the lag judgment network.

Denote l the index for the version of the free parameters. The optimization law is

$\alpha_{i,l+1} = \alpha_{i,l} + \Delta\alpha_{i,l}$, $i = 1, 2, \cdots, n_\alpha$ with

$$\Delta\alpha_{i,l} = \rho_a \Delta\alpha_{i,l-1} - \mu_a \left(\frac{\partial H_k}{\partial \alpha_i}\right)_{\alpha=\alpha_l}, \quad (36)$$

where ρ_a is the momentum constant, and μ_a is a positive learning-rate parameter. Define the judgment residual ξ_k as

$$\xi_k = \frac{1}{2}(\lambda_k^{\mathrm{D}} - \hat{\lambda}_k)^2, \quad k \in [0, K). \quad (37)$$

The learning law tries to minimize the judgment residual by carrying out the gradient decent method.

$\beta_{i,l+1} = \beta_{i,l} + \Delta\beta_{i,l}$, $i = 1, 2, \cdots, n_\beta$ with

$$\Delta\beta_{i,l} = \rho_c \Delta\beta_{i,l-1} + \mu_c \left\{\frac{\partial \Lambda(k|\beta)}{\partial \beta_i}\right\}_{\beta=\beta_l} (\lambda_k^{\mathrm{D}} - \hat{\lambda}_k), \quad (38)$$

where ρ_c is the momentum constant, and μ_c is a positive learning-rate parameter.

IV. Simulation Results of the AOCA in a FHPS-Powered Electric Sedan

This section investigates the AOCA for maturing the EMS of a FHPS-powered electric sedan. The EMS network, lead judgment network, and lag judgment network are each a RBF neural network with ten Gaussian neurons in the hidden layer [36], and each with appropriate number of inputs and outputs.

The AOCA trains the EMS network on a training set consisting of the data of five driving cycles: the Urban Dynamometer Driving Schedule (UDDS), the Highway Fuel Economy Test (HWFET), the US-06 Aggressive Driving Cycle, the New European Driving Cycle (NEDC) and the Federal Test Procedure (FTP-75). Each driving cycle provides a sequence of data points representing the speed of a vehicle versus time. The power demands of the electric sedan in the driving cycle are calculated and collected to form a training sequence. The training sequence, $\{x_0, P_L(i)\}_{i=0}^K$, contains an initial state and a sequence of power loads.

Parameters pertaining to the electric sedan and FHPS used in the test are shown in Tables I and II. The AOCA was trained in every driving cycle of the training set. Using $\theta_i = 100$ $(i = 1, 2, 3)$, the training in the driving cycle iterated until $\left|(x_K - x_0)/x_0\right| \le 0.5\%$. This termination criterion ensures that the vehicle is on average powered by the FCS. Then the obtained EMS was tested in the UDDS and US06 driving cycles while ceasing the learning/optimization laws.

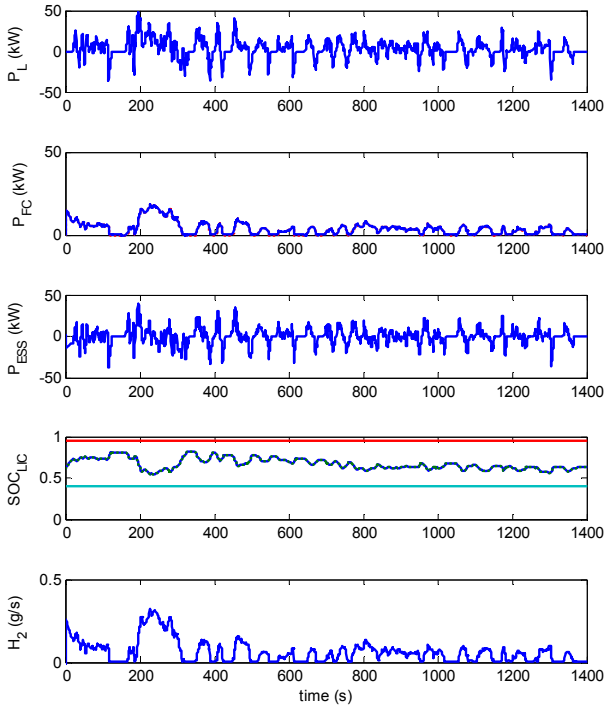

Fig. 4. Histories of energy management obtained by the EMS in the UDDS test (urban-like pattern).

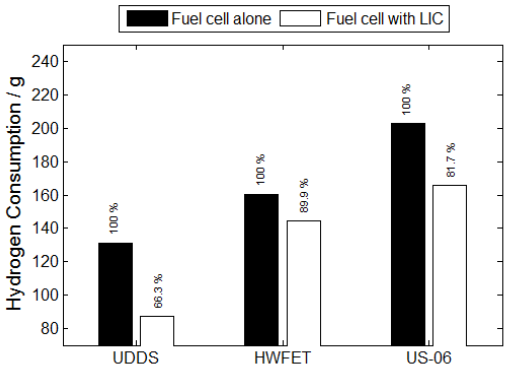

Fig. 5. The total H_2 consumptions in comparison with that supplying the sedan with the FCS alone.

1) Results of test in the UDDS driving cycle

In this test, the electric sedan is driven in an urban-like pattern, which consists of frequent accelerations and decelerations. The P_{FC} history of Fig. 4 shows that the fuel-cell power is maintained at small values. The P_{ESS} history shows that the ESS efficiently shares the power load for accelerations and captures the regenerative electricity during decelerations. The SoC history shows that the SoC shifts

toward values near 0.95 and the final SoC is nearly equal to the initial SoC. As shown in Fig. 5, the total H_2 consumption is 66.3% of that supplying the electric sedan with the FCS alone.

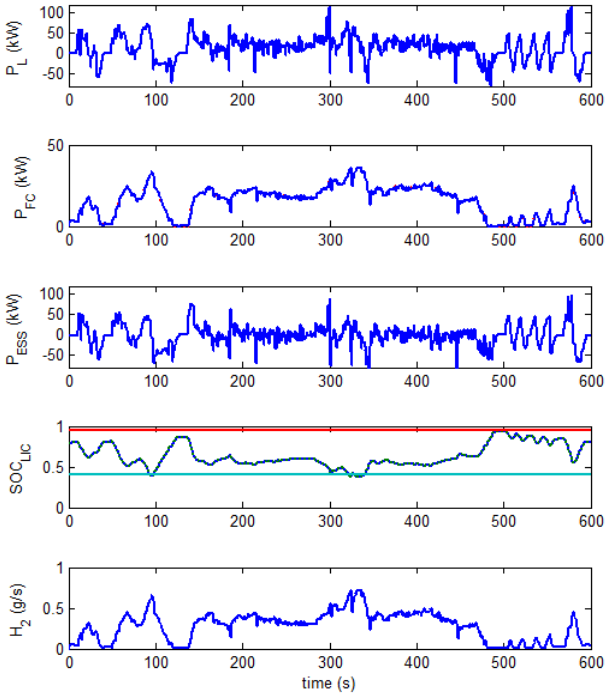

Fig. 6. Histories of energy management obtained by the EMS in the US06 test (aggressive driving pattern).

2) Results of test in the US06 driving cycle

The US06 driving cycle addresses aggressive, high speed and/or high acceleration driving behavior, rapid speed fluctuations, and driving behavior following startup. The P_L history of Fig. 6 shows that the power loads fluctuates and there are peaks larger than the maximum of the fuel-cell power. The P_{FC} history shows that the fuel-cell power is maintained at permissible values that, effectively, protects the FCS from overloading. The P_{ESS} history shows that the ESS efficiently shares the power load and captures the regenerative electricity during rapid speed fluctuations. The SoC history shows that the SoC is maintained at permissible levels and the final SoC is nearly equal to the initial SoC. Fig. 5 shows that the total H_2 consumption is 81.7% of that supplying the electric sedan with the FCS alone.

V. Conclusion

Trying to minimize fuel consumption in a FHPS-powered electric vehicle confronts a nonlinear optimization problem subject to mixed equality and inequality constraints. The AOCA made use of reinforcement learning and sequential optimization to train the EMS network in the specified driving cycles. The optimality conditions for the AOCA were derived from the minimum principle. The simulation results showed that the AOCA could offline draw out the best EMS for the FHPS-powered electric vehicle. In practical use, the AOCA is promise to operate online to fine tune the EMS. However, the detailed design for online operations of the AOCA in a FHPS-powered electric vehicle remains to be explored. The trained lead judgment network functions without reference to the model of the FCS and ESS that enables using the nominal models of the FCS and ESS to construct the parameter update laws, without sacrificing accuracy of optimization. However, model errors do influence the convergence rate of learning and optimization. Severe model errors can incur violations on the requirements for convergence of the entire system. The robustness of the AOCA against model errors remains to be studied in the future.

Table I. Parameters of the Electric Sedan

Parameter	Symbol	Value
Total mass	M	2049 kg
Air drag coefficient	C_d	0.31
Frontal area	A_f	2 m^2
Air density	R_a	1.23 kg m^{-3}
Coefficient of rolling resistance	f_r	0.01
Acceleration due to gravity	g	9.8 m s^{-2}

Table II. Parameters of the FHPS

Parameter	Symbol	Value
Maximum FCS power	$P_{FC\min}$	50 kW
Minimum FCS power	$P_{FC\min}$	5 kW
Maximum FCS rising power rate	$\Delta P_{FC,rise}$	5 kW s^{-1}
Maximum FCS falling power rate	$\Delta P_{FC,fall}$	-5 kW s^{-1}
Resistance of Li-ion capacitor/cell	R_i, R_t, R_d	1.18, 0.3, 0.9 m Ω
Capacitance of Li-ion capacitor/cell	C_d, C_p	2200, 12.1 F
Inductance of Li-ion capacitor/cell	L	0 H
Diffusion order of Li-ion capacitor/cell	n	6
Maximum SoC of Li-ion capacitor	$SoC_{\max}$	0.95
Minimum SoC of Li-ion capacitor	$SoC_{\min}$	0.35
Voltage range of Li-ion capacitor	[min, max]	[2.2, 3.8] V
Li-ion capacitor bank	Serial Parallel	44 cells 3 strings
Efficiency of boost converter	η_1	0.95
Efficiency of buck-boost converter	η_2	0.95
Coefficients of curve fitting for hydrogen consumption	(a_3 , a_2 , a_1 , a_0)= (4.1953, -2.0662, 1.6944, 0.0066)	

References

[1] H. Gualous, G. Alcicek, Y. Diab, A. Hammar, P. Venet, K. Adams, M. Akiyama, and C. Marumo, "Li-ion capacitor characterization and modelling," presented at the 3rd European Symposium on Supercapacitors and Applications, Roma, Italy, 2008.

[2] S. M. Lambert, V. Pickert, J. Holden, X. He, and W. Li, "Comparison of supercapacitor and lithium-ion capacitor technologies for power electronics applications," in *5th IET International Conference on Power Electronics, Machines and Drives*, Bringhton, UK, 2010, pp. 1-5.

[3] S. N. An, K. I. Lee, and T.-J. Kim, "Performance analysis according to the combination of energy storage system for fuel cell hybrid vehicle," *International Journal of Automotive Technology,* vol. 9, pp. 111-118, 2008.

[4] W.-S. Lin and C.-H. Zheng, "Energy management of a fuel cell/ultracapacitor hybrid power system using an adaptive optimal-control method," *Journal of Power Sources,* vol. 196, pp. 3280-3289, 2011.

[5] A. C. Baisden and A. Emadi, "ADVISOR-based model of a battery and an ultra-capacitor energy source for hybrid electric vehicles," *IEEE Trans. on Vehicular Technology,* vol. 53, pp. 199-205, 2004.

[6] T. Andersson, J. Groot, H. Berg, J. Lindstrom, and T. Thiringer, "Alternative energy storage system for hybrid electric vehicles," *Department of Electric Power Engineering Chalmers University of Technology, Master of Science Thesis,* 2003.

[7] Y. Haifang, L. Rengui, W. Tiecheng, and Z. Chunbo, "Energetic macroscopic representation based modeling and control for battery/ultra-capacitor hybrid energy storage system in HEV," in *Vehicle Power and Propulsion Conference*, 2009, pp. 1390-1394.

[8] A. Vahidi, A. Stefanopoulou, and H. Peng, "Current management in a hybrid fuel cell power system: a model-predictive control approach," *IEEE Trans. on Control Systems Technology,* vol. 14, pp. 1047-1057, NOVEMBER 2006.

[9] Q. Chen, L. Gao, R. A. Dougal, and S. Quan, "Multiple model predictive control for a hybrid proton exchange membrane fuel cell system," *Journal of Power Sources 191 (2009),* pp. 473-482, 2009.

[10] T. Zhu, S. R. Shaw, and S. B. Leeb, "Transient recognition control for hybrid fuel cell systems," *IEEE Trans. on Energy Conversion,* vol. 21, pp. 195-201, March 2006.

[11] M. Kim, Y. Sohn, W. Lee, and C. Kim, "Fuzzy control based engine sizing optimization for a fuel cell/battery hybrid mini-bus," *Journal of Power Sources 178 (2008),* pp. 706-710, 2008.

[12] C. Y. Li and G. P. Liu, "Optimal fuzzy power control and management of fuel cell/battery hybrid vehicles " *Journal of Power Sources 192 (2009),* pp. 525-533, 2009.

[13] X. Li, L. Xu, and J. Hua, "Power management strategy for vehicular-applied hybrid fuel cell/battery power system," *Journal of Power Sources 191 (2009),* pp. 542-549, 2009.

[14] G. Paganelli, T. M. Guerra, S. Delprat, J. J. Santin, M. Delhom, and E. Combes, "Simulation and assessment of power control strategies for a parallel hybrid car," *Journal of Automobile Engineering,* vol. 214, pp. 705-718, 2000.

[15] P. Rodatz, G. Paganelli, A. Sciarretta, and L. Guzzella, "Optimal power management of an experimental fuel cell/supercapacitor-powered hybrid vehicle," *Control Engineering Practice 13(2005),* pp. 41-53, 2005.

[16] D. Feroldi, M. Serra, and J. Riera, "Energy management strategies based on efficiency map for fuel cell hybrid vehicles," *Journal of Power Sources 190 (2009),* pp. 387-401, 2009.

[17] S. Delprat, J. Lauber, T. M. Guerra, and J. Rimaux, "Control of a parallel hybrid powertrain: optimal control," *IEEE Trans. on Vehicular Technology,* vol. 53, pp. 872-881, 2004.

[18] J. Bernard, S. Delprat, F. Buechi, and T. M. Guerra, "Global optimisation in the power management of a fuel cell hybrid vehicle (FCHV)," *IEEE Conference,* 2006.

[19] R. S. Sutton and A. G. Sutton, *Rinforcement learning: an introduction*. Cambridge, M.A.: MIT Press, 1998.

[20] A. Gosavi, "Reinforcement learning: a tutorial survey and recent advances," *INFORMS Information on Computing,* vol. 21, pp. 178-192, 2009.

[21] W.-S. Lin and C.-H. Zheng, "Constrained adaptive optimal control using reinforcement learning agent," *Automatica,* vol. 48, pp. 2614-2619, 2012.

[22] W.-S. Lin, "Optimality and convergence of adaptive optimal control by reinforcement synthesis," *Automatica,* vol. 47, pp. 1047-1052, 2011.

[23] P. Werbos, *Approximate dynamic programming for real-time control and neural modeling. Handbook of Intelligent Control*: White and Sofge, Eds. New York: Van Nostrand Rein-hold., 1992.

[24] L. S. Pontryagin, V. G. Boltyanskii, R. V. Gamkrelidze, and E. F. Mishenko, *The mathematical theory of optimal processes vol. 4: Translation of a Russian book ISBN 2881240771*, 1962.

[25] R. Bellman, *Dynamic programming*. N.J., USA: Princeton University Press, 1957.

[26] I. Takahashi and Y. Ohmori, "High-performance direct torque control of an induction motor," *IEEE Trans. on Industry Applications,* vol. 25, pp. 257-264, 1989.

[27] D. V. Prokhorov, "Toyota Prius HEV neuralcontrol and diagnostics," *Neural Networks,* vol. 21, pp. 458-465, 2008.

[28] S. S. Rao, *Engineering optimization theory and practice, 4th edition*: John Wiley & Sons, 2009.

[29] K. B. Wipke, M. R. Cuddy, and S. D. Burch, "ADVISOR 2.1: a user-friendly advanced powertrain simulation using a combined backward/forward approach," *IEEE Trans. on Vehicular Technology,* vol. 48, pp. 1751-1761, 1999.

[30] C. Y. Li and G. P. Liu, "Optimal fuzzy power control and management of fuel cell/battery hybrid vehicles," *Journal of Power Sources,* vol. 192, pp. 525-533, 2009.

[31] A. M. Dhirde, N. V. Dale, H. Salehfar, A. D. Mann, and T.-H. Han, "Equivalent electric circuit modeling and performance analysis of a PEM fuel cell stack using impedance spectroscopy," *IEEE Trans. on Energy Conversion,* vol. 25, pp. 778-786, 2010.

[32] S. V. Puranik, A. Keyhani, and F. Khorrami, "State-space modeling of proton exchange membrane fuel cell," *IEEE Trans. on Energy Conversion,* vol. 25, pp. 804-813, 2010.

[33] H. Gualous, G. Alcicek, Y. Diab, A. Hammar, P. Venet, K. Adams, M. Akiyama, and C. Marumo, "Li-ion capacitor characterization and modelling," presented at the 3rd European Symposium on Supercapacitors and Applications, Roma, Italy, Nov. 2008.

[34] F. Lewis and V. Syrmos, *Optimal control*. New York: Wiley Inc., 1995.

[35] B. C. Kuo, "Digital control systems, Chapter 11," 2nd edition ed New York: Saunders College Publishing, 1992.

[36] S. Haykin, *Neural networks and learning machines, 3rd edition*. Hong Kong: Pearson, 2009.